Chapter 4
Remote Sensing of Car Tire Pressure

Thomas Herndl

Abstract State-of-the-art tire pressure monitoring systems (TPMS) are wireless sensor nodes mounted on the rim. Attaching the node on the inner liner of a tire allows sensing of important additional technical parameters, which may be used for improved tracking and engine control, feedback to the power train and car-to-car communication purposes. Thus a significant step in car control appears feasible. Those new features come at a price: the maximum weight of the sensor is limited to 5 g including package, power supply, and antenna. Robustness is required against extreme levels of acceleration of up to 3,000 g ($g = 9.81\,\mathrm{m/s^2}$). The node size is limited to about $1\,\mathrm{cm^3}$ to avoid high force gradients due to device deformation and finally, a 10-year power supply lifetime must be achieved. In this chapter we present a self-sufficient tire-mounted wireless sensor node.

- with a bulk acoustic wave (BAW)-based low-power FSK transceiver;
- pioneered for an energy scavenger-based low-volume and low-weight power supply; and
- a 3D vertical chip stack for best compactness, lowest volume, and highest robustness for pressure, inertia, and temperature sensing.

Keywords TPMS · Tire pressure monitoring system · Energy harvesting · Energy scavenging · Wireless sensor network · 3D system integration · Sensor system

4.1 Motivation for Tire Pressure Monitoring Systems

More than 20 years have passed since in 1986 the Porsche 959 car was first equipped with a built-in tire pressure monitoring system (TPMS) [1] and since then millions of cars have followed, because of the large variety of safety risks surrounding incorrectly inflated or damaged tires. In fact, underinflated tires are more prone to stress damage, have less lateral traction, a shorter tread life, and are more vulnerable to flat tires and blowouts (Fig. 4.1).

T. Herndl (✉)
Infineon Technologies Austria AG, Vienna, Austria
e-mail: thomas.herndl@infineon.com

T.J. Kaźmierski, S. Beeby (eds.), *Energy Harvesting Systems*,
DOI 10.1007/978-1-4419-7566-9_4,

Fig. 4.1 Tire blowout

Furthermore, underinflated tires can increase the distance required for a vehicle to stop, particularly at wet surface conditions. Investigations in the USA have shown that

1. one-fifth of all tires are up to 40% under their correct pressure;
2. 10% drop in pressure cuts a tire's service life by 15%;
3. each 0.2 bar drop in pressure increases fuel consumption by 1.5%;
4. 75% of flat tires due to insufficient pressure or gradual pressure loss;
5. tire problems are third most common cause of vehicle breakdowns; and
6. ~250,000 accidents a year (the USA) can be traced back to insufficient tire pressure.

Thus, triggered by the US National Highway Traffic Safety Administration (NHTSA) recent laws have put the spotlight on the issue of tire pressure monitoring. The 2000 TREAD (Transportation Recall Enhancement, Accountability, and Documentation) Act requires automobile manufacturers to gradually provide TPMS for all cars sold in the USA [2, 3]. As minimum requirements a "low tire pressure" indication lamp and a "malfunction" indication lamp have been defined (Fig. 4.2).

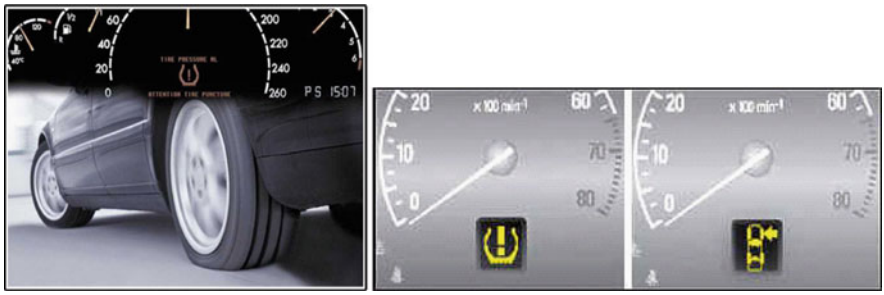

Fig. 4.2 Obligatory in the USA: low tire pressure indication and malfunction indicators

While for the time being in Europe TPMS is rather considered as non-mandatory comfort feature, it is very likely that automotive manufacturers will be obliged by law to equip new cars with TPMS, starting from 2013.

4.2 Overview of State-of-the-Art TPMS

State-of-the-art direct tire pressure monitoring systems (TPMS) are wireless sensor nodes mounted on the rim. Basically, there are mainly three technologies competing for their market presence.

4.2.1 Direct Battery-Based (Active) Systems

Direct battery-based (active) systems have their own independent power source integrated in the modules and each module contains a pressure sensor. The modules are mounted on the rim, as part of the valve (Fig. 4.3). Core functions (sensors and wireless transmitter) are integrated into a system in package (SiP). In order to fulfill lifetime requirements, the battery size is quite large and dominates the total weight and size of the TPMS module.

Only a single, central radio-receiver is required (Fig. 4.4), which is typically located in the dashboard. All in all this keeps the total system costs moderate. Due

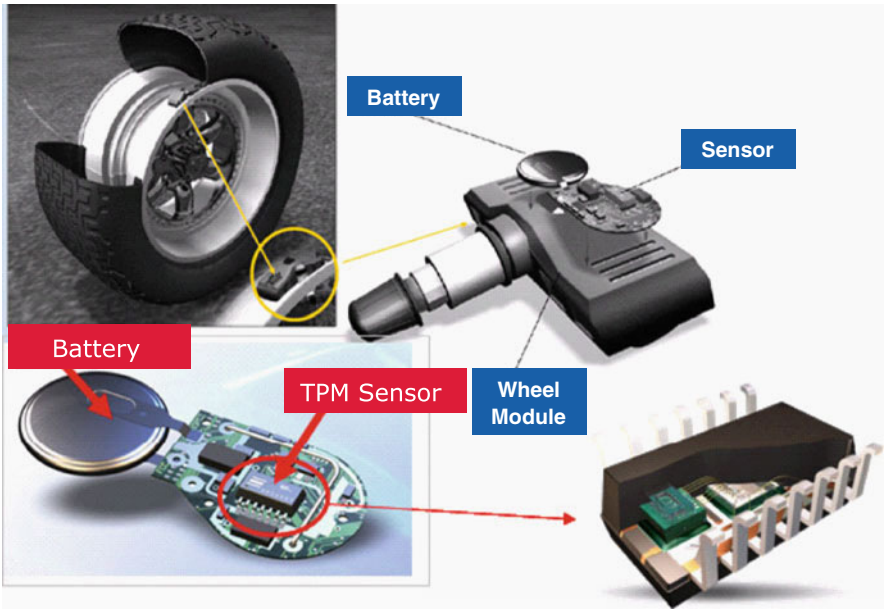

Fig. 4.3 Rim-mounted tire pressure monitoring system and subcomponents (state of the art)

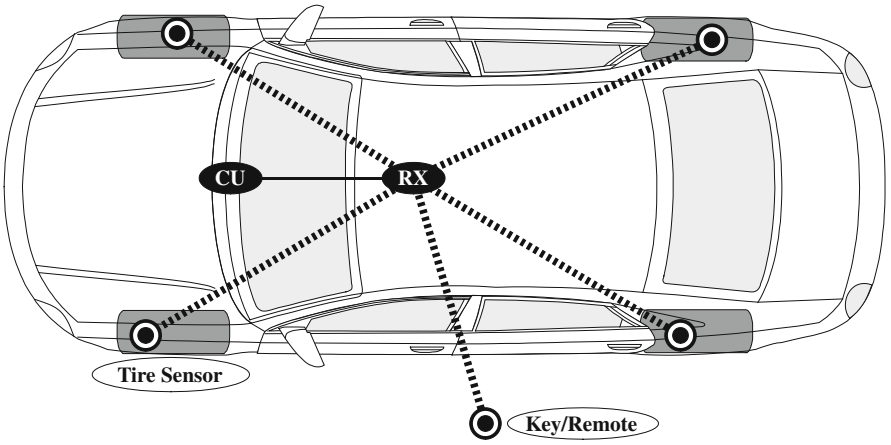

Fig. 4.4 Tire pressure monitoring system communicating with ECU/dashboard in a star network topology

to their superior performance figures at moderate costs, direct battery-based systems constitute far the major share among all available technologies for tire pressure monitoring.

4.2.2 Direct Battery-Less (Passive) Systems

Direct battery-less (passive) systems do not have a power source, rather they are powered by an external reader device by means of an electromagnetic field. They contain a pressure sensor. While the sensor modules are cheap, direct battery-less systems have high total systems cost, as they require a powering/reader device in the vicinity of each wheel, e.g., in the wheelhouse, which complicates the wiring for connectivity and increases the bill of material (BOM).

4.2.3 Indirect (ABS-Based) Systems

Indirect (ABS-based) systems do not contain a pressure sensor. They rely on an SW approach by using ABS data (wheel speed sensors) and evaluate the relative number of turns among the wheels, based on the fact that a lower inflated tire has a smaller roll radius/circumference than a higher inflated one. Logically, they offer the cheapest total system costs, but at the expense of accuracy and comfort: Indirect systems cannot measure absolute pressure. They need initial calibration and regular re-calibration by the driver and it takes several minutes for first tire pressure notifications upon engine start during normal operation.

Due to the position of the sensor node in the valve, the node has only very loose contact to the road surface, which prevents additional important parameters from

being monitored. Hence, state-of-the-art rim-mounted direct systems, equipped in many (US) cars, have limited sensing capabilities, restricted to movement detection, tire pressure and tire temperature monitoring. Further on, the rim-mounted TPMS node "does not intrinsically know" which tire it carries, hence it is not possible to trustworthily report even "simple" additional tire-specific static information, like a tire-ID reflecting the mounted tire type (summer/snow tires; spikes), which would be a very valuable parameter for the ABS system to further optimize the stopping distance of the vehicle in emergency situations. Indeed, additional parameters can be reported when moving the TPMS module to within the tire, as shown in Fig. 4.5.

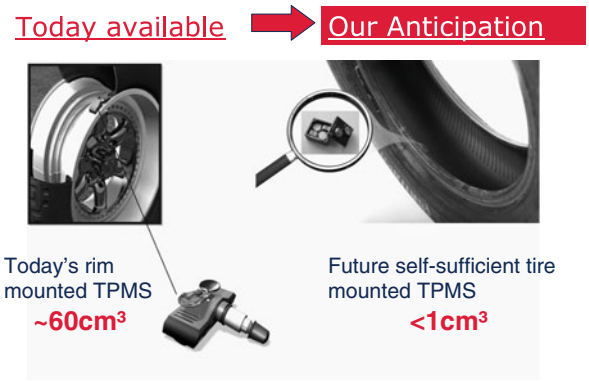

Fig. 4.5 Rim-mounted versus in-tire-mounted TPMS module

4.3 Motivation and Requirements for In-Tire TPMS

Attaching the TPMS node on the inner liner of a tire allows the extraction of additional information for comfort and safety beyond tire pressure and temperature, such as

- vehicle load;
- wheel speed;
- wear;
- tire friction, side slip, road condition; and
- integrated tire-ID for logistic purposes (fleet management, localization, automatic detection of tire change, and tire type for input to ABS).

They may be used for improved tracking and engine control, feedback to the power train and car-to-car communication purposes and can therefore contribute to further enhance driving safety.

Technically, additional parameters can be derived from acceleration signals occurring at the border between the road surface and the tire. As can be seen from Fig. 4.6, which shows signal traces measured with an acceleration sensor attached

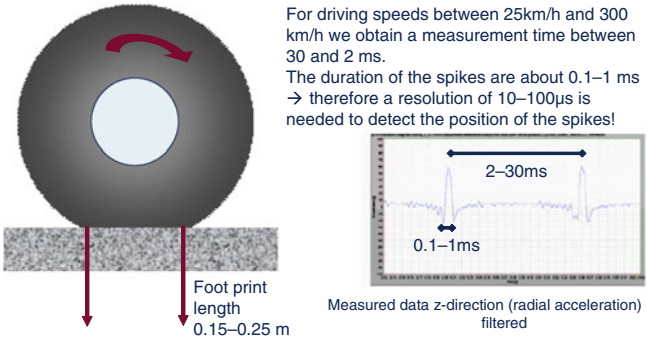

Fig. 4.6 Technical background for additional in-tire parameter monitoring: acceleration signal trace from the tire

at the inner liner of the tire, two steep negative acceleration peaks and one dominant positive acceleration peak in between can be observed: the first negative peak occurs at positions when the tire-attached sensor touches down at the road surface and the second peak when it lifts up again. By proper measurement of the positive peak duration (respectively, the time between the two negative peaks) and the distance between the positive peaks, one can calculate the footprint length and other important parameters listed above. Additionally the same mechanical shock signal can be used as the source for a vibration harvesting unit, translating mechanical power into electric power for supplying a self-sufficient, battery-less sensor node.

Those new features come at a price: The maximum weight of the in-tire sensor is limited to ∼5 g including package, power supply, and antenna. Robustness is required against extreme levels of acceleration of up to 3,000 g ($g = 9.81\,\mathrm{m/s^2}$). The node size is limited to about $1\,\mathrm{cm^3}$ to avoid high force gradients due to device deformation and finally, a 5- to 10-year power supply lifetime must be achieved.

4.4 A Self-Sufficient In-Tire TPMS Demonstrator

In this chapter we present a self-sufficient tire-mounted wireless sensor node. Figure 4.7 shows a block diagram of the in-tire TPMS demonstrator, consisting of a MEMS sensor, a power supply module, a microcontroller ASIC, and a transceiver ASIC which directly generates the RF carrier by using a BAW resonator.

The key innovations of the demonstrator are

- a bulk acoustic wave (BAW)-based frequency shift keying (FSK) transceiver;
- pioneered for an energy scavenger-based low-volume and low-weight power supply;
- a 3D vertical chip stack for best compactness, lowest volume, and highest robustness; and
- molded interconnect device (MID) package solution with integrated antenna

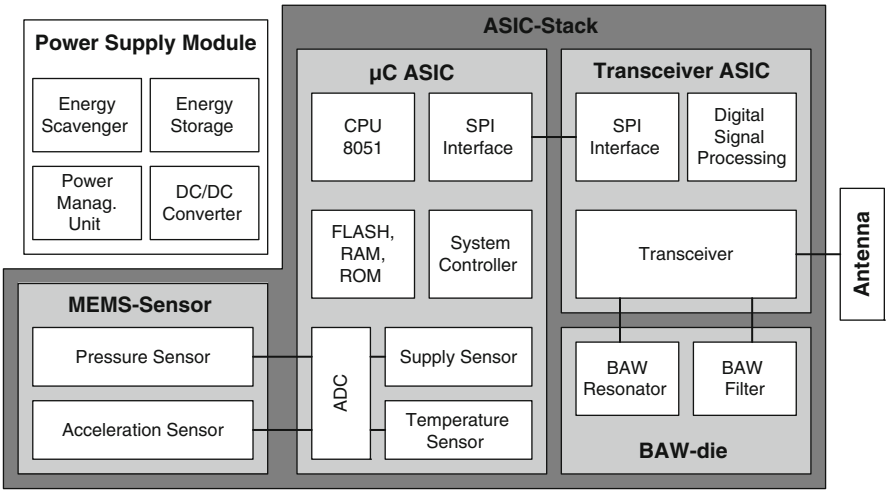

Fig. 4.7 Block diagram of the in-tire TPMS sensor node demonstrator

for pressure, inertia, and temperature sensing and will be presented in more detail in the following.

4.4.1 RF Transceiver

For use in the proposed sensor node a BAW-based RF transceiver has been developed (Fig. 4.8), which directly generates a 2.4 (2.11) GHz carrier (two variants have been designed, operating at carrier frequencies of 2.11 and 2.4 GHz) by using a BAW resonator with a size of only 0.02 mm^2. It avoids the employment of a bulky and shock-sensitive crystal and a phase-locked loop (PLL), which makes the system more robust and radically reduces the turn-on time to a few microseconds from several milliseconds as in state-of-the-art crystal oscillator systems. This improves the overall power consumption [1, 4].

For the receiving section an image-reject architecture has been chosen with BAW resonators integrated into the LNA for filtering [5]. Typically the parasitic capacitances of the electrodes of the BAWs are not equal, since the bottom electrodes have a higher capacitance against substrate. Therefore it is advantageous to use two BAWs, one in each branch of the differential LNA. Since the attenuation near the series resonance frequency of the BAW is very high, low side injection of the local oscillator (LO) signal leads to a high additional suppression of the image frequency, allowing for a low intermediate frequency (IF) of 10.7 MHz. In contrast to [6], the presented receiver utilizes the narrow bandwidth of a single BAW resonator instead of a filter consisting of several resonators. The LNA is followed by an RC polyphase network to generate the I- and Q-phases for the image-reject mixer. At the IF the received signal is filtered and fed into a limiting amplifier delivering a binary signal,

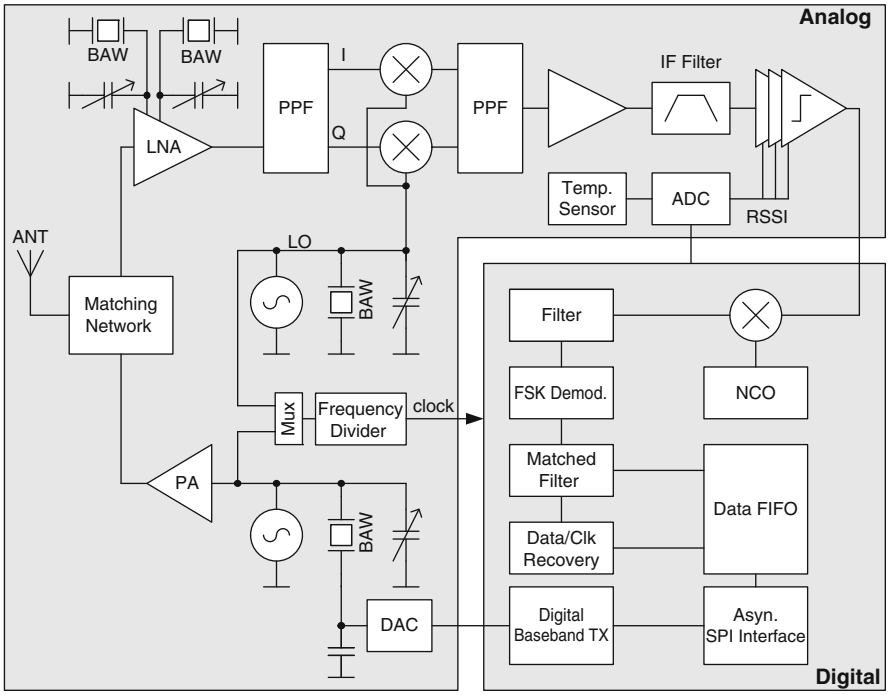

Fig. 4.8 Block diagram of the BAW transceiver

which is directly mixed into complex baseband in the digital domain. After digital filtering, demodulation, and de-framing the received payload is stored in a FIFO.

Small-sized shock-resistant BAW resonators are utilized as frequency reference for the TRX and channel selection filter in the receive chain [7]. A BAW resonator can be considered as a thin film of piezoelectric material sandwiched between two metal electrodes. When an electric field is applied between the electrodes, the structure is mechanically deformed by way of inverse piezoelectric effect and acoustic waves are launched into the bulk of the device [8].

Basically two approaches can be distinguished to prevent that the resonant energy is not absorbed by the carrier substrate. In the first one, micromachining is used to generate a membrane. The second approach is shown in Fig. 4.9, where the waves are reflected on an acoustic mirror and therefore cannot propagate any further into the substrate [8]. The benefits offered by a BAW resonator includes extremely high mechanical robustness, higher quality factor (Q) than surface acoustic wave (SAW) devices or on-chip LC tanks, small size, and lower temperature dependency and higher ESD robustness than SAW.

One major drawback of BAW devices is their temperature dependency, which is typically in the range of $-18\,\mathrm{ppm}/^{\circ}\mathrm{C}$ (Fig. 4.10).

To overcome temperature drift effects the temperature is measured and compensated via digitally controlled capacitors (9 bit) in parallel to the resonator in

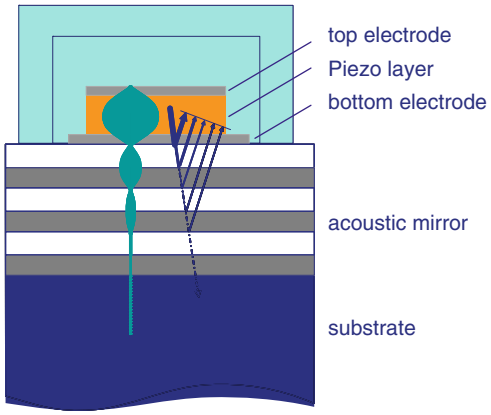

Fig. 4.9 Basic concept of a BAW resonator with acoustic mirror

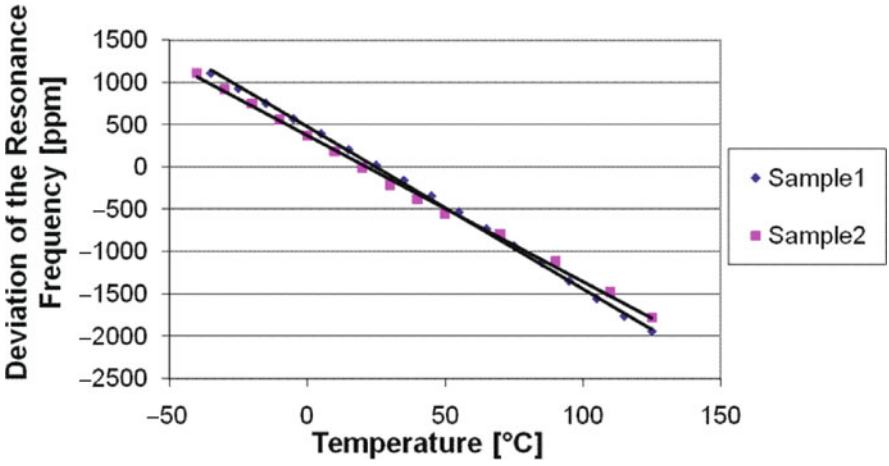

Fig. 4.10 Temperature dependency of the BAW device resonance frequency without temperature compensation

the range of −40 to +125°C. Figure 4.11 shows the resulting frequency deviation which stays within ±40 ppm for the whole temperature range after applying a proper temperature compensation algorithm. Additionally, the BAW can be tuned with a variable DC biasing, which causes a change in the stiffness of the piezoelectric BAW material. The biasing voltage causes a linear frequency shift with a slope of 40 kHz/V. Due to the fast response of the resonator, this effect is used for FSK modulation in the transmitter. Direct carrier modulation and frequency tuning are also possible with the digitally controlled tuning capacitors, but the nonlinear and process-dependent relationship between capacitance and resonance frequency is a drawback, which has to be considered when applying this method.

The transceiver ASIC was fabricated by using a 0.13 µm standard, automotive-qualified CMOS process. Its current consumption is 6 mA in transmit mode at a

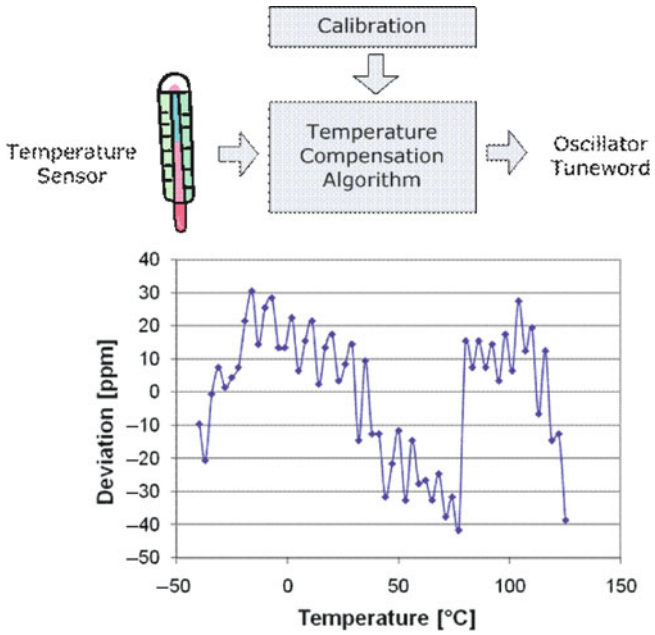

Fig. 4.11 Temperature dependency of the BAW device resonance frequency with applied temperature compensation algorithm

transmit output power of 1 d Bm and 8 mA in receive mode with a sensitivity of −90 dBm at a data rate of 50 kb/s. The turn-on time of the transceiver is only 2 µs.

4.4.2 Power Supply Subsystem

The power supply subsystem (Fig. 4.12) consists of

- miniaturized MEMS transducer device;
- high efficient power translation ASIC (0.25 µm automotive-qualified CMOS process);
- external coil for the inductive AC/DC converter; and
- energy storage device (low-leakage capacitor).

For the MEMS vibration scavenger an electrostatic transducer device has been chosen, manufactured by using high aspect ratio micromachining (Fig. 4.13) [9].

It already integrates an electret for biasing of the transducer; hence, there is no additional external voltage source required. Due to the very small mass of the miniaturized vibration scavenger and the resulting very weak mechanical coupling, only a small portion of the available mechanical energy in the tire can be actually translated into electrical energy. In-tire measurements and electromechanical simulations have shown that the scavenging system with a vibrating mass of about 30 mm^2 is able

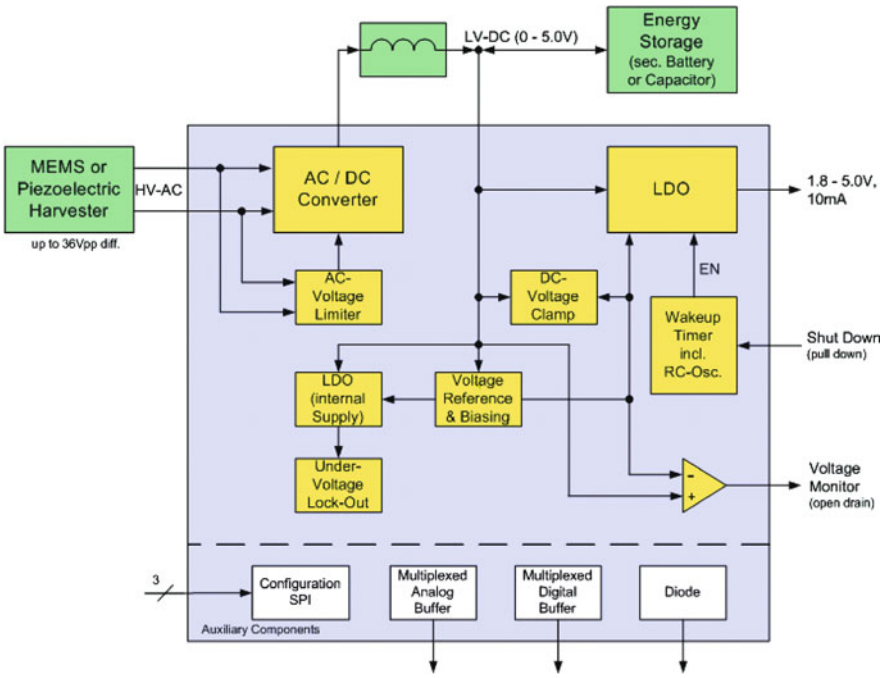

Fig. 4.12 Block diagram of the vibration scavenger-based power supply subsystem

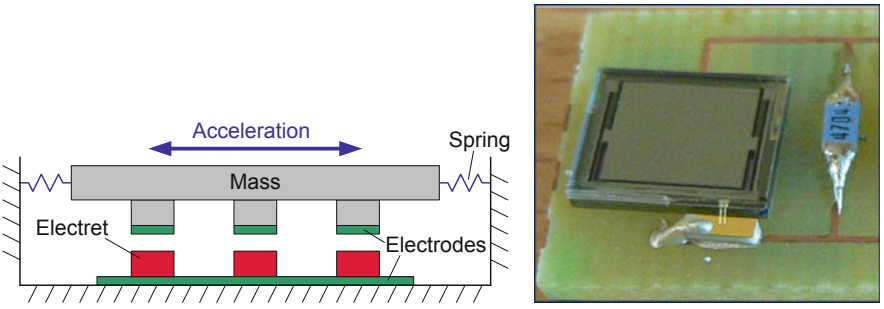

Fig. 4.13 Vibration scavenger: functional principle (*left*) and photo of the device (*right*)

to deliver some microamperes at 50 km/h driving speed, which is sufficiently high for regular reporting of the tire pressure at appropriate intervals. With increasing driving speed, the available vibration power also increases, allowing for shortening the reporting intervals, which results in higher update rates for pressure reports at higher driving speeds.

The successive power conversion ASIC integrates a high efficient inductive AC/DC down-converter for charging a capacitor up to the desired voltage level. It can process AC input voltages up to ~40 V. The input stage of the harvester interface consists of an active full bridge rectifier with peak detector. The peak detector

generates the optimum trigger time instant for voltage conversion, independent of the output voltage. Once the switch has been turned on, down-conversion is done within a "single shot" via the external coil. Upon completion of the conversion cycle, the harvester's capacitance is discharged and starts recharging again with opposite polarity due to mechanical oscillation. Therefore, the amount of conversion cycles is minimized for high power efficiency at lowest switching losses. An additional low drop output (LDO) voltage regulator is used to remove a potential ripple voltage at the output of the AC/DC converter. Further on, the ASIC provides auxiliary and control circuitry that are used for output voltage monitoring and switching off and switching on of the output power supply system. It makes sure that the output voltage is switched on once a certain voltage level is reached. Alternatively the integrated wake-up timer, making use of an ultra-low power 2 kHz RC oscillator, can be used for interval-based duty cycling of the power system. For the in-tire TPMS demonstrator the power supply is regularly switched on after exceeding a certain energy level (respectively, voltage level) available in the capacitor (low-leakage ceramic capacitor with $C = 200\,\mu F$), which has been properly dimensioned to ensure that sufficient energy can be stored for at least one pressure measurement and reporting cycle. A capacitor was used for energy buffering, as alternative secondary battery technologies suitable for harshest environmental conditions as present in the tire (high temperatures and high mechanical forces at the same time) are not available in the market.

4.4.3 Overall System Integration of the In-Tire TPMS Node

For demonstration purposes, both a battery-driven and a vibration harvester-driven version have been designed. In order to reach high compactness and robustness for system integration, miniaturization concepts have been applied on different levels.

Figure 4.14 shows a sketch of the overall integration concept for the battery version. For the scavenger-driven version another micro-PCB has been designed,

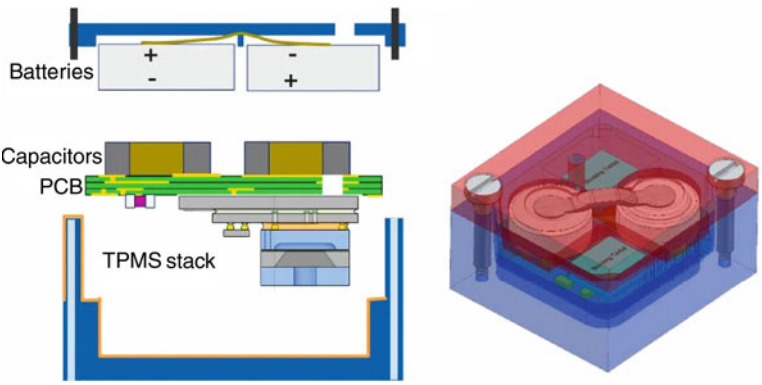

Fig. 4.14 Sketch of the overall integration concept for the battery-driven TPMS demonstrator

which replaces the lid. The space of the batteries and the capacitors is used for the placement of all subcomponents of the scavenger power supply subsystem.

All functional core components such as microcontroller, transceiver, BAW device, and sensor were co-assembled by means of 3D vertical system integration, making use of through silicon vias (TSV), applied to the RF transceiver ASIC and the sensor, and bumping technologies [10–13]. The resulting 3D sub-stack shown in Fig. 4.15 was glued and wire-bonded onto a micro-PCB (Fig. 4.16). At the opposite side of this micro-PCB tiny cell batteries and buffer capacitors were placed for the battery-driven version.

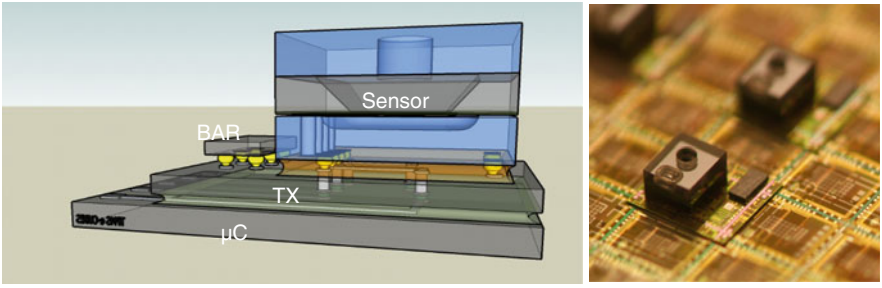

Fig. 4.15 Sketch and photo of the TPMS 3D chip sub-stack (*source*: SINTEF)

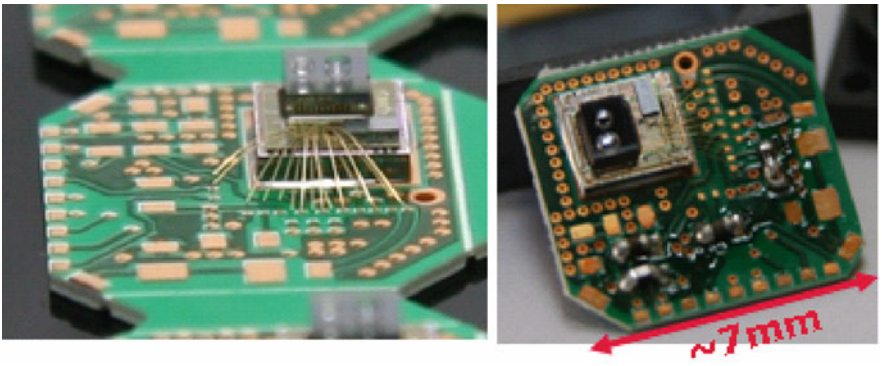

Fig. 4.16 TPMS 3D chip sub-stack assembled on the micro-PCB

For packaging, a cube-like plastic 3D substrate was designed using MID technology (molded interconnect device, Fig. 4.17), allowing for integration of conducting lines directly onto the package surface. This ability was beneficially used for shaping a loop antenna and providing the connectivity between the functional TPMS subsystem and the power supply subsystem. The overall dimensions of the MID package are only $1.2 \times 1.3 \times 0.64\,\text{cm}^3 = 0.998\,\text{cm}^3$, which is less than $1\,\text{cm}^3$.

Figure 4.17 shows the lid with metal springs used for the battery-driven version. For the scavenger-driven version a micro-PCB of the same size as the lid was

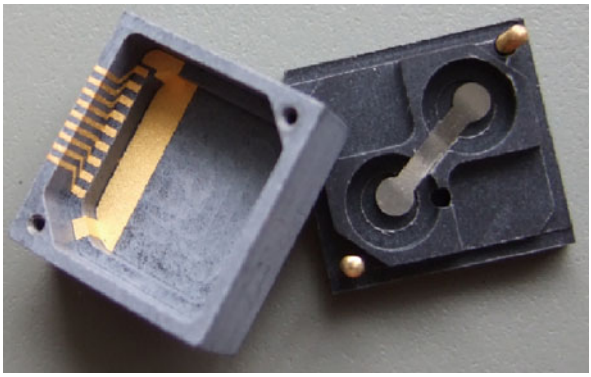

Fig. 4.17 MID package for the TPMS sensor node demonstrator

used, comprising all subcomponents of the scavenger power supply (Fig. 4.18) as described in Section 4.4.2.

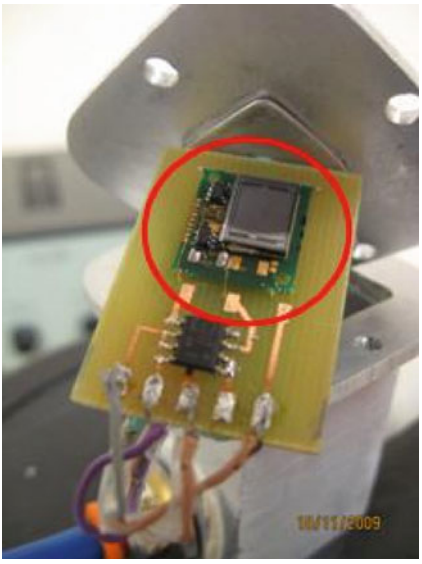

Fig. 4.18 Vibration harvester power supply board of the in-tire TPMS demonstrate

Figures 4.19 and 4.20 finally present different views of the fully assembled TPMS demonstrator node (battery version and harvester version, respectively); the hole in the MID package serves as pressure inlet. The transparent package shown in Fig. 4.19 has been designed for visualization purposes only and is not functional.

Based on the fully assembled TPMS demonstrators, system characterization has been performed. One key performance parameter is the overall power consumption, respectively, energy consumption. Figure 4.21 shows the measured current profile for a system cycle (pressure measurement and reporting). Three

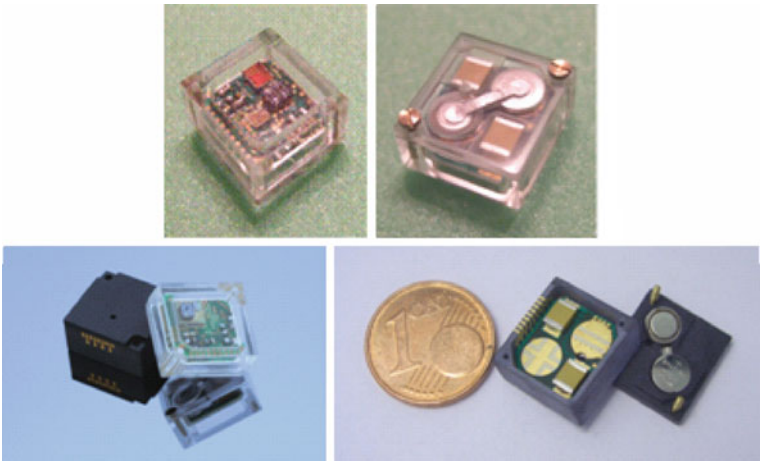

Fig. 4.19 Fully assembled TPMS demonstrator (battery version)

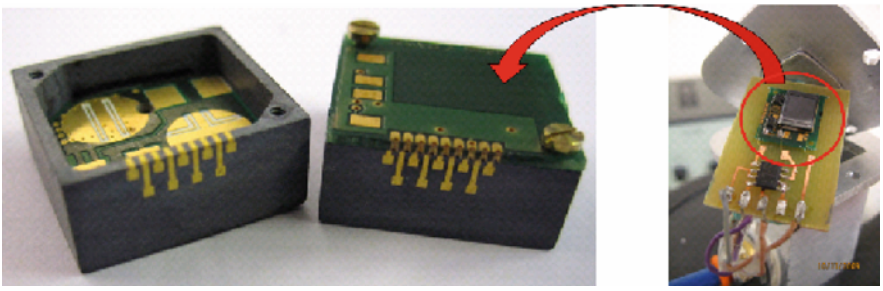

Fig. 4.20 Fully assembled TPMS demonstrator (vibration scavenger version)

phases can be observed: Upon activation of a system cycle, the pressure value is sensed and post-processed by the microcontroller. After completion of the sensor measurement phase the system is configured for the following data transmission. A temperature measurement is done and temperature compensation of the RF frequency is performed (see also Fig. 4.11). Further on, the RF transmitter is properly configured. Finally, the data are transmitted over the wireless channel, which terminates the reporting cycle. This is done in a cyclic manner.

One whole cycle requires about 5 ms. The average current consumption over the active cycle is about 5 mA. When activating the cycle every 10 s, the average current consumption significantly drops down to about 3 μA, which can be delivered by the vibration scavenging power supply system at driving speeds of $\sim$50 km/h. When driving at lower speeds, the reporting interval needs to be prolonged, as it takes longer to charge the storage capacitor due to the diminished electrical power from the harvester.

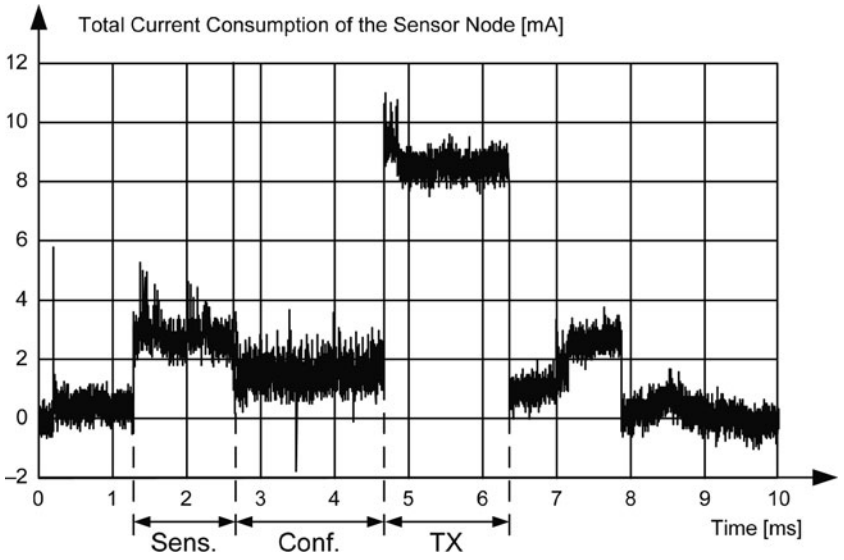

Fig. 4.21 Current consumption profile of the in-tire TPMS demonstrator for a measurement and data reporting cycle

Technology	
Transceiver	CMOS, 0.13µm
Microcontroller	CMOS, 0.24µm
Current Consumption	
Oscillator core + biasing	900uA
Transmitter, 1dBm	6mA
Receiver, -90dBm, 50kBit/s	8mA
Overall peak current	<10mA

Fig. 4.22 Key performance figures of the in-tire TPMS demonstrator

Figure 4.22 summarizes key performance figures of the in-tire TPMS demonstrator. It shall be emphasized that at no time the overall current consumption exceeds 10 mA, which relaxes the requirements for the power supply system significantly.

4.5 Outlook and Future Work

The presented results of this industrial case study have demonstrated feasibility of a self-sufficient, robust, miniaturized in-tire TPMS module. Based on these results, extended functions as described in Section 4.3 can introduce further added value without creating significant extra system costs, as the vibration scavenger output signal can be reused for deriving complementary physical parameters by means of appropriate algorithms running on an embedded microcontroller.

From a system point of view, TPMS as pioneering reference application for an automotive wireless sensor network (WSN) has high potential to pave the way toward extended intra-vehicle WSN functions. An intra-vehicle WSN could provide a solution for integrating and connecting the growing number of sensor functions within modern vehicles. Particularly non-safety critical sensor functions are suitable candidates for wireless connection. An extended intra-vehicle WSN can

- simplify the ever more and more complex cable tree and therefore
- reduce system costs by eliminating connectors to either or both data communication lines and board battery power system
- contribute to the reduction of overall vehicle weight by omitting cables (in modern cars there are some kilometer cable lengths installed)
- add more flexibility in comparison to a wire-based solution and create added value by making new sensing and monitoring applications possible at locations which are cumbersome or even inaccessible for wire-based access (e.g., at rotating parts and wheels)
- exhibit multicast topology by nature – based on neighborhood – and can therefore provide redundancy and diversity, hence can add reliability – in contrast to wire-based connections – without extra wiring costs

Intra-vehicle WSN technology should not be considered as competitive technology to existing wired field bus systems like CAN, LIN, FlexRay, to name a few; rather the idea is to complement wired solutions and to partially get rid of cables. In particular this includes the ever-growing area of passenger comfort functions, e.g., the penetration of automatic, multi-zone, and high-efficiency climate control systems is increasing and thus the demand for temperature sensors will increase as well. Particularly such "quasi-static" types of sensors with relaxed data rate and update rate demands could be powered by energy harvesters to reach energy autonomy over years, which is a crucial requirement for a future successful automotive WSN roll-out scenario.

4.6 Conclusion

The presented industrial case study has demonstrated the feasibility of a vibration scavenger-driven, highly miniaturized in-tire-mounted TPMS module. By applying careful low power system design and employing robust technology building blocks, proper interconnect technologies and packaging solutions, a volume $< 1\ \text{cm}^3$ for the whole TPMS module, including power supply, at lowest weight could be achieved without compromising performance and reliability issues. The results obtained from this case study can be taken as a cornerstone toward "intelligent tires," which would be able to measure and report additional technical parameters for further enhancement of road safety.

Acknowledgments The presented work has been performed in the course of the European EC-FP6 funded project *e-Cubes*. Web page: http://www.ecubes.org; Contact: Thomas Herndl (thomas.herndl@infineon.com – Graz/Austria) and Werner Weber (werner.weber@infineon.com – Munich/Germany). Special thanks go to Martin Flatscher (Infineon Technologies Austria AG – Graz/Austria), Markus Dielacher (Infineon Technologies Austria AG – Graz/Austria), Josef Prainsack (Infineon Technologies Austria AG – Graz/Austria), Rainer Matischek (Infineon Technologies Austria AG – Graz/Austria), for their excellence in RF transceiver development and demo system integration; Jakob Jongsma (Infineon Technologies Austria AG – Graz/Austria) for his precious technical guidance, Mohammed Abd Allah (Infineon Technologies AG – Munich/Germany) for his highly relevant work on BAW device-level temperature compensation, Horst Theuss (Infineon Technologies AG – Regensburg) for development and design of the packaging solution, and Shi Cheng (Uppsala University – Uppsala/Sweden) for integrated antenna design. Technology development for vertical chip integration, design and implementation of the 3d-Sensor/ASIC stack assembly has been done by Fraunhofer IZM Munich and Berlin, SINTEF, IMEC and SensoNor; particularly many thanks go to Peter Ramm (Fraunhofer IZM – Munich/Germany), Josef Weber (Fraunhofer IZM – Munich/Germany), Jürgen Wolf (Fraunhofer IZM – Berlin/Germany), Maaike M. V. Taklo (SINTEF – Oslo/Norway), Nicolas Lietaer (SINTEF – Oslo/Norway), Eric Beyne (IMEC – Leuven/Belgium), Walter De Raedt (IMEC – Leuven/Belgium), and Terje Kvisteroey (Sensonor – Horten/Norway). Finally, integration of the harvester power supply system would not have been possible without the key components provided by Austrian FIT-IT-funded Project ***PAWiS*** (FFG-No. 810194), conducted by TU Vienna/Institute of Computer Technology and Infineon Technologies Austria AG; Web page: http://www.ict.tuwien.ac.at/pawis Contact: Stefan Mahlknecht (mahlknecht@ict.tuwien.ac.at) Christian Hambeck (hambeck@ict.tuwien.ac.at) and Norwegian RCN Project No. 176485 *Nanomaterials for micro energy harvesting* conducted by Infineon Technologies Sensonor, SINTEF and Vestfold University College Contact: Einar Halvorsen (einar.halvorsen@hive.no).

References

1. Ludvigsen K. (2003) Porsche. Excellence Was Expected, vol. 3. Bentley Publishers, Cambridge, MA, p 1011
2. Otis B et al (June 2004) An ultra-low power MEMS-based two-channel transceiver for wireless sensor network. VLSI Circuits
3. Kowalewski M (August–September 2004) Monitoring and managing tire pressure. IEEE Potentials 23(3):8–10
4. Dubois MA (July 2–4, 2003) Thin film bulk acoustic wave resonators: a technology overview. In: 4th Workshop on MEMS for Millimeterwave Communications, MEMSWAVE 2003, Toulouse, France
5. Dielacher M, Flatscher M, Pribyl W (July 2009) A low noise amplifier with on-chip matching network and integrated bulk acoustic wave resonators for high image rejection. In: Research in Microelectronics and Electronics, 2009. PRIME 2009. Ph.D., Cork, Ireland, pp 172–175
6. Chabloz J et al (February 6–9, 2006) A low power 2.4 GHz CMOS receiver front-end using BAW resonators. In: Solid State Circuits Conference ISSCC 2006. Digest of Technical Papers. IEEE International, San Francisco, CA, pp 1244–1253
7. Flatscher M, Dielacher M, Herndl T, Lentsch T, Matischek R, Prainsack J, Pribyl W, Theuss H, Weber W (February 2009) A robust wireless sensor node for in-tire-pressure monitoring. In: Solid-State Circuits Conference – Digest of Technical Papers, 2009. ISSCC 2009, IEEE International, San Francisco, CA, US, pp 286–287,287a
8. Flatscher M, Dielacher M, Herndl T, Lentsch T, Matischek R, Prainsack J, Pribyl W, Theuss H, Weber W (January 2010) A bulk acoustic wave (baw) based transceiver for an in-tire-pressure monitoring sensor node. Solid-State Circuits, IEEE J. 45:167–177
9. Ramm P, Klumpp A, Weber J, Taklo M (December 2009) 3D System-on-Chip Technologies for More than Moore systems; P. Ramm, A. Klumpp, J. Weber, M. Taklo;

Journal of Microsystem Technologies (Springer), p. 1–5; Published online: Dec 18, 2009 http://www.springerlink.com/content/3n84397t82263112/ DOI 10.1007/s00542-009-0976-1, ISSN: 1432–1858 (Online)
10. Lietaer N et al (October 4–9, 2009) Meet. Abstr. – Electrochem. Soc./MA2009-02/216th ECS Meeting. In: 3D Interconnect Technologies for Advanced MEMS/NEMS Applications – An Invited Talk, Vienna, Austria
11. Schjølberg-Henriksen K et al (2009) Miniaturised sensor node for tire pressure monitoring (e-CUBES). In: Advanced Microsystems for Automotive Applications – Smart Systems for Safety, Sustainability, and Comfort, Meyer G, Valldorf J, Gessner W (eds.). Springer, Berlin, pp 313–332
12. Halvorsen E, Westby ER, Husa S, Vogl A, Østbø NP, Leonov V, Sterken T, Kvisterøy T (June 21–25 2009) An electrostatic energy harvester with electret bias. In: The IEEE 15th International Conference on Solid-State Sensors, Actuators & Microsystems, Transducers, 2009, pp 1381–1384, Denver, CO
13. Lietaer N, Taklo M, Klumpp A, Weber J, Ramm P (November 2009) 3D integration technologies for miniaturized tire pressure monitor systems (TPMS). San Jose, CA, US. In: Proceedings of 42nd International Symposium on Microelectronics – IMAPS 2009